Corrections to the strong-stretching theory of polymer brushes due to the proximal layer

ARTICLE *in* THE JOURNAL OF CHEMICAL PHYSICS · FEBRUARY 2003

Impact Factor: 2.95 · DOI: 10.1063/1.1539089

Corrections to the strong-stretching theory of polymer brushes due to the proximal layer

M. W. Matsen[a] and J. M. Gardiner
Polymer Science Centre, University of Reading, Whiteknights, Reading RG6 6AF, United Kingdom

(Received 26 August 2002; accepted 25 November 2002)

Proximal-layer corrections to the strong-stretching theory (SST) for polymer brushes are tested against self-consistent field theory (SCFT). The corrections qualitatively account for a number of significant differences between SST and SCFT occurring next to the substrate. This includes severe deviations away from the parabolic field normally predicted by SST, and nonzero slopes in the single-chain segment distributions. When SST is also combined with corrections for the end-segment entropy, the quantitative agreement with SCFT becomes impressive, particularly in regards to the self-consistent field and the stretching energy of individual chains. © *2003 American Institute of Physics.* [DOI: 10.1063/1.1539089]

I. INTRODUCTION

When polymer chains are grafted to a substrate in high concentrations, they are forced to extend away from the substrate forming a so-called brush.[1] Polymer brushes provide not only a useful way of modifying surface properties, but also a valuable testing ground for polymeric theories. With this latter purpose in mind, we examine the simple system of two opposing brushes as illustrated in Fig. 1. Provided the polymers are of high molecular weight, they can be accurately modeled as Gaussian chains, effectively treating them as microscopic elastic threads.[2] The hard-core interactions, which normally prevent polymer chains from overlapping, can be accounted for by invoking a mean field, $w(z)$, determined self-consistently so as to produce a uniform polymer density.

The complete self-consistent field theory (SCFT) for such a system was formulated by Edwards in 1965.[3] However, this approach requires a numerical calculation.[4,5] To allow for analytical calculations, the theory is generally simplified by assuming the chains are stretched so much that they are unable to deviate from their lowest-energy configurations referred to as *classical* trajectories. The resulting strong-stretching theory (SST), developed by Semenov[6] and by Milner *et al.*,[7] provides remarkably simple predictions. First of all, it predicts that the two brushes in Fig. 1 remain completely separated with none of the chains ever crossing the $z=L$ midplane. On the left-hand side (i.e., $0\leqslant z\leqslant L$), the self-consistent field acquires the well-known parabolic dependence,

$$w(z)=-\frac{3\pi^2 z^2}{8a^2N}, \tag{1}$$

where N is the number of segments in each chain, and a is the statistical segment length. The polymer trajectories take on the form,

$$z_\alpha(s)=z_0\cos(\pi s/2), \tag{2}$$

where $0\leqslant s\leqslant 1$ is a parameter running uniformly along the length of a chain, and z_0 is the chain extension. The corresponding segment distribution for a chain with its free end at z_0 is

$$\phi(z;z_0)=\begin{cases}\dfrac{2aN^{1/2}}{\pi\sqrt{z_0^2-z^2}} & \text{if } 0\leqslant z<z_0\\ 0 & \text{if } z_0<z.\end{cases} \tag{3}$$

Given that, the distribution of the chain ends must satisfy

$$g(z_0)=\begin{cases}\dfrac{z_0}{L\sqrt{L^2-z_0^2}} & \text{if } 0\leqslant z_0<L\\ 0 & \text{if } L<z_0\leqslant 2L,\end{cases} \tag{4}$$

so that the incompressibility requirement,

$$\int_0^{2L} g(z_0)\phi(z;z_0)dz_0=1, \tag{5}$$

is obeyed for all $0\leqslant z\leqslant L$. The expressions for the brush on the right (i.e., $L\leqslant z\leqslant 2L$) are completely analogous.

Although SST provides nice simple expressions that have greatly aided our general understanding of polymer brushes, direct comparisons with SCFT reveal that the analytical predictions are extremely inaccurate for realistic conditions (i.e., $L/aN^{1/2}\sim 1$). On the basis of SCFT calculations, the field $w(z)$ is far from parabolic particularly near the substrates where, in fact, it is not even monotonic.[8] There is also considerable interpenetration between the opposing polymer brushes causing the end-segment distribution, $g(z_0)$, to extend far beyond the midplane.[8,9] Furthermore, the polymers fluctuate considerably from their classical trajectories,[8,10] contrary to the basic assumption of SST.

In a previous study,[8] we examined corrections to the classical trajectories, Eq. (2), due to entropy associated with the chain-end distribution. This results in a much improved prediction for $w(z)$, although severe discrepancies remain at the substrates. The corrections also predict nonmonotonic

[a]Author to whom all correspondence should be addressed; electronic mail: m.w.matsen@reading.ac.uk

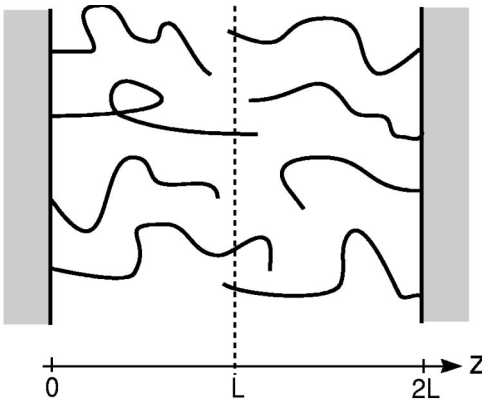

FIG. 1. Schematic diagram of two opposing brushes grafted to the substrates at $z=0$ and $2L$ such that they interpenetrate at the $z=L$ midplane denoted by the dashed line.

trajectories, $z_\alpha(s)$, and significantly alter the end-segment distribution function, $g(z_0)$, all in good agreement with SCFT. Although the end-segment-entropy corrections produce significant interpenetration of segments between the two opposing brushes, the level is still considerably less than that predicted by SCFT.

The remaining discrepancies between SST and SCFT can be attributed to fluctuations about the classical trajectories.[11] They will, undoubtedly, increase the interpenetration between the two brushes, thus further improving the agreement between SST and SCFT. It is not at all obvious that they might also correct the serious inaccuracies occurring next to the substrates. However, predictions by Likhtman and Semenov[12] for so-called proximal layers suggest that, in fact, they do. In the following, we test this through detailed comparisons with SCFT at $L/aN^{1/2}=2$.

II. THEORY

Polymer brush theory is generally based upon course-grained Gaussian chains. In this model, the energy of a chain fragment with sN segments ($0\leqslant s\leqslant 1$) subjected to a field, $w(z)$, is given by

$$\frac{E[z_\alpha;s]}{k_BT}=\int_0^s\left[\frac{3}{2a^2N}|z'_\alpha(t)|^2+w(z_\alpha(t))\right]dt, \tag{6}$$

where $z_\alpha(t)$ is the z component of its trajectory. Assuming the ends of the fragment are fixed by $z_\alpha(0)=z_0$ and $z_\alpha(s)=z$, its partition function is

$$q(z,z_0,s)\propto\int\mathcal{D}z_\alpha\exp\left\{-\frac{E[z_\alpha;s]}{k_BT}\right\}\delta(z_\alpha(0)-z_0)\times\delta(z_\alpha(s)-z), \tag{7}$$

which can be obtained by solving the modified diffusion equation,

$$\frac{\partial}{\partial s}q(z,z_0,s)=\frac{a^2N}{6}\frac{\partial^2}{\partial z^2}q(z,z_0,s)-w(z)q(z,z_0,s), \tag{8}$$

with the initial condition $q(z,z_0,0)=\delta(z-z_0)aN^{1/2}$. It is this function, $q(z,z_0,s)$, that underpins the theoretical calculations. The difference between SCFT and SST is that the former includes all possible polymer trajectories in Eq. (7), whereas the latter only includes the *classical* trajectory that minimizes Eq. (6).

With that, we are prepared to address the proximal-layer corrections, dealing with how fluctuations about the classical trajectories affect a polymer brush next to its substrate. The theory for this was developed very recently by Likhtman and Semenov,[12] but unfortunately they were unable to provide details due to page constraints. Thanks to vital information conveyed to us by the authors through private communication, we are able to present the details here.

To start, we consider a single polymer chain of N segments with one end attached at $z=0$ and the other end pulled in the positive z direction by a tension of τk_BT. The distribution of its segments is given by

$$c(z)=\frac{\int_0^1ds\int_{-\infty}^{\infty}dz_0q(0,z,1-s)q(z,z_0,s)\exp(\tau z_0)}{\int_{-\infty}^{\infty}q(0,z_0,1)\exp(\tau z_0)dz_0}. \tag{9}$$

Eventually, a substrate will be placed at $z=0$, but for now the polymer trajectories are permitted to enter the $z<0$ region. First, we derive a simpler expression for $c(z)$ in terms of two functions depending only on z. This is done by rewriting Eq. (9) as

$$c(z)=\frac{\int_0^1\Psi(z,s)q(0,z,1-s)\exp\left(\frac{a^2N}{6}\tau^2s\right)ds}{\int_{-\infty}^{\infty}q(0,z_0,1)\exp(\tau z_0)dz_0}, \tag{10}$$

where

$$\Psi(z,s)\equiv\exp\left(-\frac{a^2N}{6}\tau^2s\right)\int_{-\infty}^{\infty}q(z,z_0,s)\exp(\tau z_0)dz_0. \tag{11}$$

Since we are only concerned with $c(z)$ near the substrate, the integrand in the numerator of Eq. (10) only needs to be accurate for $s\approx 1$. In this limit, $\Psi(z,s)$ is nearly constant, allowing for the approximation,

$$c(z)\approx\frac{\Psi(z,1)}{\Psi(0,1)}\int_0^1q(0,z,1-s)\exp\left(-\frac{a^2N}{6}\tau^2(1-s)\right)ds \tag{12}$$

$$\approx\psi_1(z)\psi_2(z), \tag{13}$$

where

$$\psi_1(z)\equiv\int_0^{\infty}q(0,z,s)\exp\left(-\frac{a^2N}{6}\tau^2s\right)ds, \tag{14}$$

$$\psi_2(z)\equiv\frac{\Psi(z,1)}{\Psi(0,1)}=\frac{\int_{-\infty}^{\infty}q(z,z_0,1)\exp(\tau z_0)dz_0}{\int_{-\infty}^{\infty}q(0,z_0,1)\exp(\tau z_0)dz_0}. \tag{15}$$

Although $\psi_1(z)$ has no simple physical interpretation, $\psi_2(z)$ is the ratio of the partition function for a polymer chain with one end under tension, τk_BT, and the other end fixed at z to the partition function for a similar chain fixed, instead, to the origin. On the basis of Eq. (8), the first of these functions satisfies

$$\frac{a^2N}{6}\frac{\partial^2}{\partial z^2}\psi_1(z)=\left(\frac{a^2N}{6}\tau^2+w(z)\right)\psi_1(z)-\delta(z)aN^{1/2}, \tag{16}$$

with the two conditions, $\psi_1(\pm\infty)=0$. Similarly,

$$\frac{a^2N}{6}\frac{\partial^2}{\partial z^2}\Psi(z,s)=\left(\frac{\partial}{\partial s}+\frac{a^2N}{6}\tau^2+w(z)\right)\Psi(z,s), \quad (17)$$

from which it follows that

$$\frac{a^2N}{6}\frac{\partial^2}{\partial z^2}\psi_2(z)=\left(\frac{a^2N}{6}\tau^2+w(z)\right)\psi_2(z), \quad (18)$$

with the conditions, $\psi_2(-\infty)=0$ and $\psi_2(0)=1$.

To understand the effect of introducing a substrate at $z=0$, we begin by solving $c(z)$ for $w(z)=0$. In this case, the partition function (7) is

$$q(z_1,z_2,s)=\sqrt{\frac{3}{2\pi s}}\exp\left(-\frac{3(z_1-z_2)^2}{2sa^2N}\right). \quad (19)$$

From the definitions in Eqs. (11), (14), and (15), we then obtain

$$\psi_1(z)=\frac{3}{\tau aN^{1/2}}\exp(-\tau|z|), \quad (20)$$

$$\Psi(z,s)=\frac{aN^{1/2}}{2}\exp(\tau z), \quad (21)$$

$$\psi_2(z)=\exp(\tau z). \quad (22)$$

Notice that in this particular case, $\Psi(z,s)$ is completely independent of s. By inserting these expressions into Eq. (13), it follows that

$$c(z)=\begin{cases}\dfrac{3}{\tau aN^{1/2}} & \text{if } z>0\\ \dfrac{3}{\tau aN^{1/2}}\exp(2\tau z) & \text{if } z<0.\end{cases} \quad (23)$$

In the case of flexible chains, a substrate at $z=0$ can be treated by applying reflecting boundary conditions, and thus the concentration of segments becomes $c(z)+c(-z)$. This reflection produces an elevated concentration of segments next to the substrate in a region, $0\leqslant z\lesssim(2\tau)^{-1}$, referred to as the *proximal* layer.[12] Provided that the tension is high, the width, $\mu\equiv(2\tau)^{-1}$, of this layer will be relatively narrow.

Ultimately, the total segment profile in the brush must be uniform near the substrate, which is not possible if there is a discontinuity in $c'(z)$ at $z=0$ as predicted by Eq. (23). The only way to eliminate such a kink is to apply an infinite potential at $z=0$. Thus, we assume the field for a polymer brush has the following form:

$$w(z)=w_0(z)+\frac{a^2N}{3}\beta\delta(z)+w_r(z), \quad (24)$$

where $w_0(z)$ is the parabolic potential given by Eq. (1) and $w_r(z)$ is a proximal-layer correction that approaches zero for $z\gg\mu$. Furthermore, we assume the thickness, L, of the brush is sufficiently large that $w_0(z)\approx 0$ within the proximal layer.

Therefore, we now compute $c(z)$ for $w(z)\approx\Delta w(z)\equiv(a^2N/3)\,\beta\delta(z)+w_r(z)$. Note that $w_r(z)$ must be an even function, because of the reflecting boundary condition at $z=0$. Rather than solving $\psi_1(z)$ and $\psi_2(z)$ using their integral definitions, we now resort to the differential equations (16) and (18). By integrating Eq. (16) from $-\varepsilon$ to ε, we obtain the condition

$$\frac{a^2N}{6}[\psi_1'(\varepsilon)-\psi_1'(-\varepsilon)]=\frac{a^2N}{3}\beta\psi_1(0)-aN^{1/2}, \quad (25)$$

assuming ε is a positive infinitesimal number. Similarly for Eq. (18), we require

$$\frac{a^2N}{6}[\psi_2'(\varepsilon)-\psi_2'(-\varepsilon)]=\frac{a^2N}{3}\beta\psi_2(0). \quad (26)$$

With that, the discontinuity in $c'(z)$ is given by

$$c'(\varepsilon)-c'(-\varepsilon)=(\psi_1'(\varepsilon)-\psi_1'(-\varepsilon))\psi_2(0)+\psi_1(0)\times(\psi_2'(\varepsilon)-\psi_2'(-\varepsilon)) \quad (27)$$

$$=4\beta\psi_1(0)\psi_2(0)-\frac{6}{aN^{1/2}}\psi_2(0) \quad (28)$$

$$=4\beta c(0)-\frac{6}{aN^{1/2}}. \quad (29)$$

In a real polymer brush, the chains in the proximal layer will possess a distribution, $\nu(\tau)$, of tensions. Therefore, the requirement that the total segment concentration has zero slope at the substrate demands that

$$\beta=\frac{3}{2\langle c(0)\rangle aN^{1/2}}, \quad (30)$$

where the angular brackets denote an average over $\nu(\tau)$. Ultimately, the finite part of the potential, $w_r(z)$, will be chosen such that $\langle c(z)+c(-z)\rangle$ is uniform. The eventual value of this average can be determined by noting that $c(z)\to 3/\tau aN^{1/2}$ and $c(-z)\to 0$ for $z\gg\mu$. With that knowledge, we can evaluate $\langle c(0)\rangle$ giving us the result,

$$\beta=\langle\tau^{-1}\rangle^{-1}. \quad (31)$$

Analogous to the previous definition, the characteristic width of the proximal layer is given by $\mu\equiv(2\beta)^{-1}$.

The next step is to evaluate $w_r(z)$, which has to be done numerically. Before doing so, we scale the following quantities:

$$z=\mu\bar{z}, \quad (32)$$

$$\tau=\frac{1}{\mu}\bar{\tau}, \quad (33)$$

$$w(z)=\frac{a^2N}{6\mu^2}\bar{w}(\bar{z}), \quad (34)$$

$$\psi_1(z)=\frac{6\mu}{aN^{1/2}}\bar{\psi}_1(\bar{z}), \quad (35)$$

$$\psi_2(z)=\bar{\psi}_2(\bar{z}), \quad (36)$$

so as to remove their explicit dependence on μ. The previous differential equations for $\psi_1(z)$ and $\psi_2(z)$ now become

$$\bar{\psi}_1''(\bar{z})=(\bar{\tau}^2+\bar{w}_r(\bar{z}))\bar{\psi}_1(\bar{z}), \quad (37)$$

$$\bar{\psi}_2''(\bar{z})=(\bar{\tau}^2+\bar{w}_r(\bar{z}))\bar{\psi}_2(\bar{z}) \quad (38)$$

for $\overline{z}\neq 0$. Their respective kinks at $\overline{z}=0$ are given by

$$\overline{\psi}_1'(\varepsilon)-\overline{\psi}_1'(-\varepsilon)=\overline{\psi}_1(0)-1, \tag{39}$$

$$\overline{\psi}_2'(\varepsilon)-\overline{\psi}_2'(-\varepsilon)=\overline{\psi}_2(0)=1. \tag{40}$$

Note that, on the basis of symmetry, $\overline{\psi}_1(\overline{z})$ must be an even function. To solve these equations for a given $\overline{\tau}$, we start with an initial guess for $\overline{\psi}_1'(-\varepsilon)$ and $\overline{\psi}_2'(-\varepsilon)$. From Eq. (39), it follows that $\overline{\psi}_1(0)=1-2\overline{\psi}_1'(-\varepsilon)$. Next, we integrate $\overline{\psi}_1(\overline{z})$ and $\overline{\psi}_2(\overline{z})$ in the negative $\overline{z}$ direction until $\overline{w}_r(\overline{z})\approx 0$. From there on, the two functions should satisfy $\overline{\psi}_1'(\overline{z})=\overline{\tau}\overline{\psi}_1(\overline{z})$ and $\overline{\psi}_2'(\overline{z})=\overline{\tau}\overline{\psi}_2(\overline{z})$, but they will not, because we only guessed $\overline{\psi}_1'(-\varepsilon)$ and $\overline{\psi}_2'(-\varepsilon)$. Therefore, we adjust the two later quantities using the Newton–Raphson algorithm such that the two former conditions are satisfied. Then it is just a straightforward matter of evaluating $\overline{\psi}_2'(\varepsilon)$ with Eq. (40), integrating $\overline{\psi}_2(\overline{z})$ in the positive $\overline{z}$ direction, and calculating $\overline{c}(\overline{z})\equiv\overline{\psi}_1(\overline{z})\overline{\psi}_2(\overline{z})$. By repeating this procedure over the necessary range of $\overline{\tau}$, we can then evaluate $\langle\overline{c}(\overline{z})+\overline{c}(-\overline{z})\rangle$. This scaled version of the average segment concentration should have a uniform value of 1. If it does not, then we add a small fraction of the deviation from 1 to $\overline{w}_r(\overline{z})$, and keep repeating the calculation until $\langle\overline{c}(\overline{z})+\overline{c}(-\overline{z})\rangle=1$ to within some acceptable error tolerance.

The extra field due to the proximal layer, $\Delta w(z)$, will change the stretching energy of each chain by

$$\frac{\Delta f_{0,e}}{k_BT}=\ln\Big[\lim_{z\to\infty}\psi_2(z)\exp(-\tau z)\Big]-\frac{1}{aN^{1/2}}\int_{-\infty}^{\infty}\Delta w(z)c(z)dz. \tag{41}$$

This expression is obtained by recalling that $\psi_2(z)$ is the ratio of partition functions for two chains under tension, τk_BT, one attached to the point z and the other to the substrate. If we multiple this by $\exp(-\tau z)$ to account for the extra energy the first chain loses by its relative displacement under the constant tension and take the natural logarithm, then we get the difference in their total free energies. Taking the limit, $z\to\infty$, gives the complete free energy contribution due to the proximal layer. Finally, the energy due to the field is removed, leaving us with just the stretching energy contribution, $\Delta f_{0,e}$.

III. RESULTS

We begin by considering the basic SST, where the classical trajectories, $z_\alpha(s)$, are specified by Eq. (2) and the chain-end distribution, $g(z_0)$, satisfies Eq. (4). In this case, the tension, τk_BT, at the grafted end of a chain with its free end at z_0 is given by

$$\tau=\frac{3}{a^2N}z_\alpha'(1)=\frac{3\pi z_0}{2a^2N}=\frac{\tau_{\max}z_0}{L}, \tag{42}$$

where $\tau_{\max}=3\pi L/2a^2N$ represents the maximum tension. Since $\tau\propto z_0$, it follows that

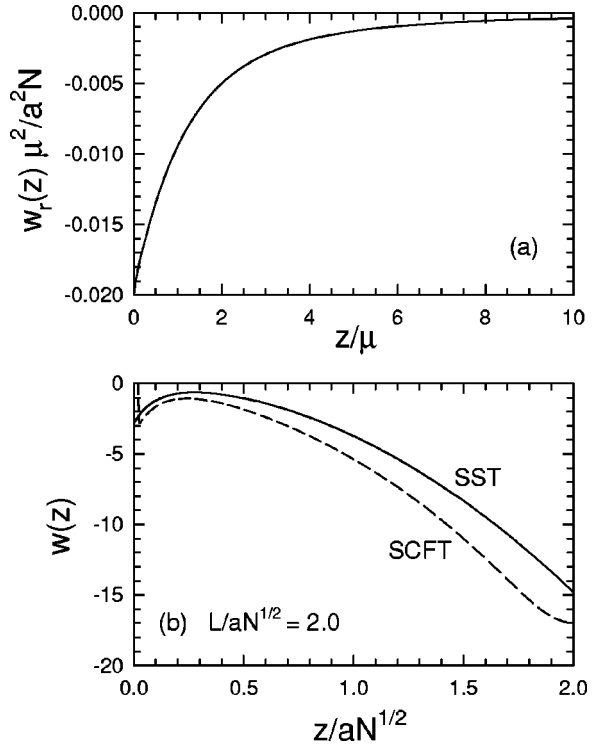

FIG. 2. (a) Proximal-layer correction to the field, $w_r(z)$, scaled with respect to the width of the proximal layer, μ. (b) SST and SCFT fields, $w(z)$, for a brush of thickness $L/aN^{1/2}=2$ shown with solid and dashed curves, respectively.

$$\nu(\tau)=\frac{\tau}{\tau_{\max}\sqrt{\tau_{\max}^2-\tau^2}} \tag{43}$$

takes on the same functional form as the end-segment distribution, $g(z_0)$, in Eq. (4). It then follows from Eq. (31) that the width of the proximal layer is

$$\mu\equiv\frac{1}{2\beta}=\frac{\pi}{4\tau_{\max}}=\frac{a^2N}{6L}. \tag{44}$$

Given $\nu(\tau)$ and μ, we calculate $w_r(z)$ following the algorithm outlined near the end of Sec. II. Figure 2(a) displays the result scaled with respect to μ. Below that, Fig. 2(b) combines $w_r(z)$ with the parabolic potential, Eq. (1), for the particular case of $L/aN^{1/2}=2$, and compares the SST result (solid curve) with SCFT (dashed curve). Although the agreement is not exceptional, the proximal-layer correction, $w_r(z)$, properly captures the qualitative behavior next to the substrate.

The SCFT field in Fig. 2(b) shows the base of a sharp peak at $z=0$. If the SCFT calculation, performed previously in Ref. 8, had attached the chains rigidly to the substrate, then this peak would become infinitesimally narrow, consistent with the delta-function term in Eq. (24). However, the chains were instead attached with stiff springs so as to avoid a true delta function and the numerical difficulties associated with it.[4] Even still, the area under the SCFT peak, $0.95aN^{1/2}$, agrees well with the SST prediction, $\beta a^2N/6=L/2=aN^{1/2}$.

Figure 3(a) plots the proximal-layer correction, $c(z)+c(-z)$, for segment profiles of individual chains, scaled

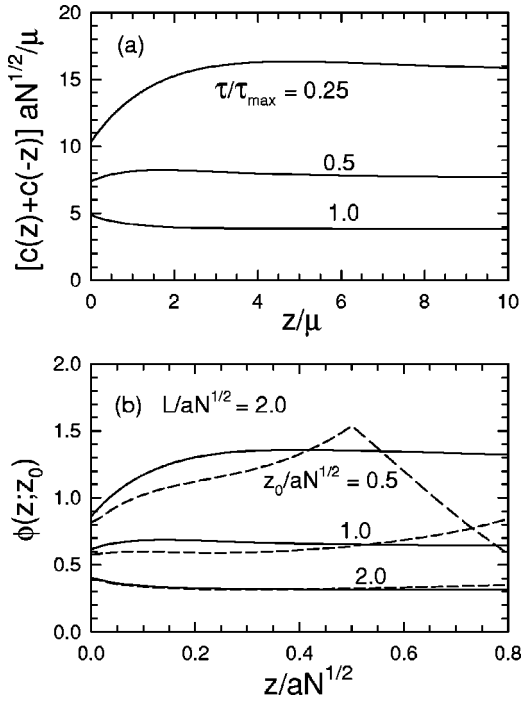

FIG. 3. (a) Segment profiles near the substrate for individual chains under various tensions, scaled with respect to the width of the proximal layer, μ. (b) SST and SCFT segment profiles, $\phi(z;z_0)$, for chains with several different extensions, z_0, within a brush of thickness $L/aN^{1/2}=2$, shown with solid and dashed curves, respectively. Note that these SST results are only meant to be accurate for $z \ll z_0$, where Eq. (3) would otherwise predict a relatively uniform distribution.

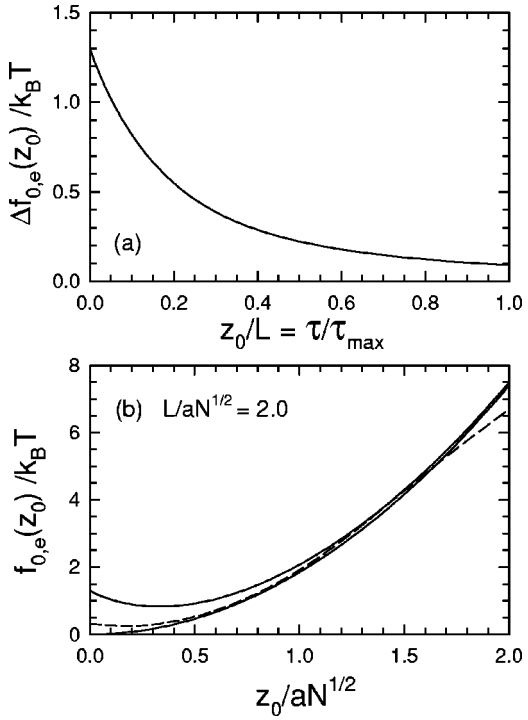

FIG. 4. (a) Proximal-layer correction for the stretching energy, $\Delta f_{e,0}(z_0)$, as a function of the chain extension, z_0. (b) Stretching energy, $f_{e,0}(z_0)$, for chains within a brush of thickness $L/aN^{1/2}=2$. The lower and upper solid curves are the uncorrected and corrected SST predictions, respectively, while the dashed curve is the SCFT result to within an additive constant.

with respect to μ. Note that this correction is only meant to apply in the proximal layer, where SST normally predicts a relatively uniform distribution,

$$\phi(z;z_0) \approx \frac{2aN^{1/2}}{\pi z_0} = \frac{3}{\tau aN^{1/2}}, \tag{45}$$

according to Eq. (3). In contrast, the corrected SST results in Fig. 3(a) show a surplus of segments next to the substrate from the highly stretched chains while there is a depletion from the lesser stretched ones. Figure 3(b) compares this proximal-layer correction with SCFT for a brush of thickness $L/aN^{1/2}=2$, and indeed this behavior is confirmed. However, the proximal-layer correction does tend to fail as $\tau \to 0$ (i.e., small z_0), for fairly obvious reasons that we will discuss later.

The most important aspect of the proximal-layer correction is its effect on the stretching energy of the brush. Figure 4 shows the predicted stretching-energy correction, $\Delta f_{0,e}$, for individual chains as a function of their extension, z_0, or alternatively their tension next to the substrate, $\tau k_B T$. Integrating this over the end-segment distribution function gives an average stretching-energy correction per chain of

$$\frac{\Delta f_e}{k_B T} = \int_0^L \frac{f_{0,e}(z_0)}{k_B T} g(z_0) dz_0 = 0.1544, \tag{46}$$

as quoted previously in Ref. 12. In Fig. 4(b), we compare the uncorrected and corrected stretching energies (solid curves) for individual chains in a brush of thickness $L/aN^{1/2}=2$ against SCFT (dashed curve). Note that SCFT only provides a relative stretching energy, and thus any vertical shift between the curves should be ignored. Unfortunately, the difference in shape between the SST and SCFT curves, if anything, increases when the proximal-layer correction is applied.

The lack of quantitative agreement can be partially attributed to inaccuracies in $\nu(\tau)$. Previous studies[8,9] have demonstrated that the entropy associated with the chain ends has a sizable effect on both $w_0(z)$ and $g(z_0)$. Not surprisingly, it also has a substantial effect on $\nu(\tau)$. Figure 5 shows $\nu(\tau)$ corrected for the end-segment entropy compared to that predicted by Eq. (43) for $L/aN^{1/2}=2$.

Switching to the revised $\nu(\tau)$ in Fig. 5, the width of the proximal layer decreases slightly to $\mu/aN^{1/2}=0.0781$. Using

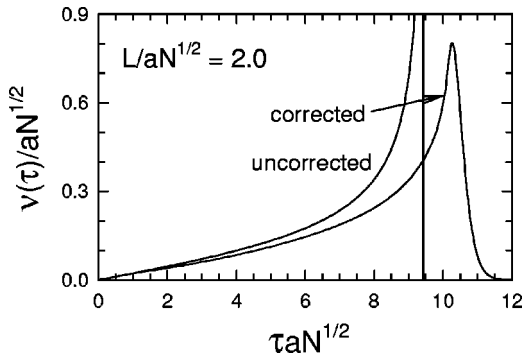

FIG. 5. Distribution of chain tensions, $\nu(\tau)$, at the substrate of a polymer brush of thickness $L/aN^{1/2}=2$. One curve shows the standard result in Eq. (43), and the other is corrected for end-segment entropy (Ref. 8).

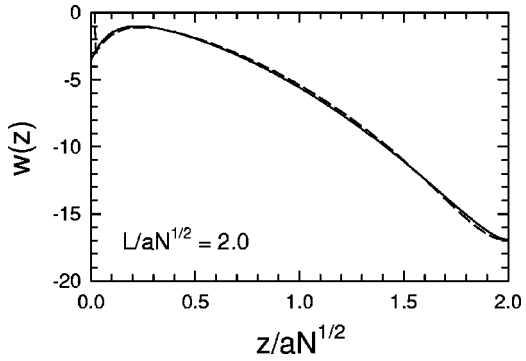

FIG. 6. Same as Fig. 2(b), except that the SST result (solid curve) is corrected for end-segment entropy.

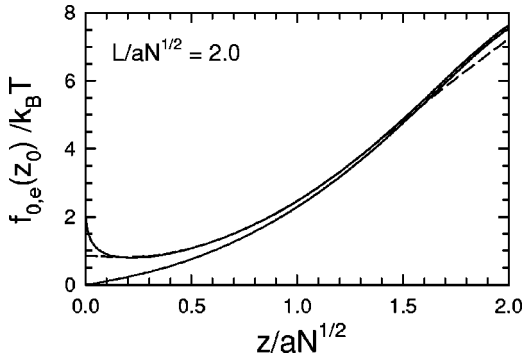

FIG. 8. Same as Fig. 4(b), except that the SST results (solid curves) are corrected for end-segment entropy.

the new $\nu(\tau)$ and μ, we now recalculate $w_r(z)$, $c(z)+c(-z)$, and $\Delta f_{0,e}(z_0)$ for a brush of thickness $L/aN^{1/2}=2$. With both corrections, the SST field agrees remarkably well with the SCFT prediction, as demonstrated in Fig. 6. From Fig. 7, we see that the segment distribution also improves for $z_0/aN^{1/2}=1.0$, although the agreement is still poor for the weakly stretched chains. Most satisfying is the fact that now, according to Fig. 8, the SST prediction for $f_{0,e}(z_0)$ agrees well with SCFT, other than for $z_0/aN^{1/2} \lesssim 0.1$. This failure at small z_0 will be discussed in Sec. IV. Reevaluating Eq. (46) with the revised $f_{0,e}(z_0)$ and $g(z_0)$, we find the average increase in stretching energy per chain due to the proximal layer is $\Delta f_e/k_BT=0.1507$, which is close to the value obtained without the end-segment corrections.

IV. DISCUSSION

Ideally, we would like to compare the SST corrections with SCFT up to the point where the uncorrected results in Sec. I become valid, but unfortunately numerical limitations prevented SCFT calculations beyond $L/aN^{1/2}\approx 2$. Nevertheless, this thickness already exceeds typical experimental conditions.[9] So, in reality, comparisons at moderate values such as $L/aN^{1/2}=2$ represent the most relevant test. If the SST corrections are to be of any value, they must provide reasonable accuracy for conditions characteristic of experiment.

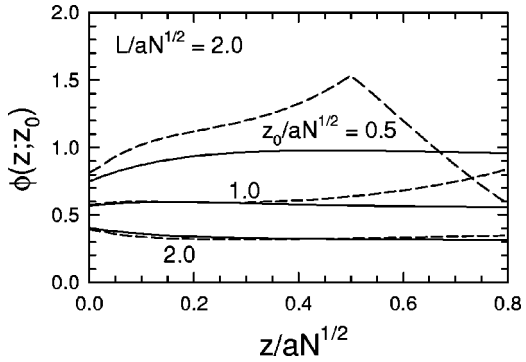

FIG. 7. Same as Fig. 3(b), except that the SST results (solid curves) are corrected for end-segment entropy.

The proximal-layer corrections, as they stand, will ultimately fail if $L/aN^{1/2}$ becomes too small. This is because they assume $w_0(z)$ is relatively constant in the interval where $w_r(z)$ significantly deviates from zero. On the basis of a 10% criterion, z must exceed 4μ [see Fig. 4(a)] before it surpasses $0.1L$ [see Eq. (1)]. This leads to the condition, $L/aN^{1/2}\gtrsim 3$, and thus we are somewhat fortunate that the proximal-layer corrections work as well as they do at $L/aN^{1/2}=2$.

Another assumption is that the proximal-layer correction for the segment distribution, $c(z)+c(-z)$, approaches its asymptotic value of $3/\tau aN^{1/2}$, before the uncorrect prediction, $\phi(z;z_0)$, in Eq. (3) deviates significantly from $3/\tau aN^{1/2}$. However, there will always be some chains that fail to meet this criterion, no matter how large we make $L/aN^{1/2}$. This explains the inaccuracy in Fig. 8 for $\Delta f_{e,0}$ when $z_0\leqslant\mu$. Fortunately, we are saved by the fact that the population of such chains is generally small. For instance, chains with $z_0\leqslant\mu$, which corresponds to $\tau \leqslant (a^2N/6L^2)\tau_{\max}$, only contribute $\sim 1\%$ toward the stretching-energy correction, Δf_e, when the brush thickness is $L/aN^{1/2}=2$.

Likhtman and Semenov[12] claim that the proximal layer represents the dominant correction for large L. Indeed, it contributes a constant correction, $\Delta f/k_BT=0.1544$, to the average energy per chain, whereas the end-segment-entropy contribution, $\Delta f/k_BT=-0.84(L/aN^{1/2})^{-2/3}$,[8] vanishes as $L\to\infty$. Nevertheless, this proximal-layer correction does not dominate until $L/aN^{1/2}\gtrsim 13$, which represents a completely unrealistic value. For thicknesses such as $L/aN^{1/2}=2$, the end-segment-entropy correction is by far the more significant, which explains why it was required to achieve quantitative agreement with SCFT.

Although the proximal-layer and end-segment-entropy corrections bring most aspects of SST into good agreement with SCFT, there is still one glaring exception. According to our previous study on end-segment-entropy corrections,[8] SST still underestimates the degree of interpenetration between the two opposing brushes, and of course the proximal-layer corrections will do nothing to improve upon this. What we need is one last correction that accounts for fluctuations about the classical trajectories much like the proximal-layer corrections do, but this time at the outer edge of the brush. We suggest that this might be accomplished by exploiting analogies with quantum mechanics as outlined by Milner.[10]

V. CONCLUSIONS

We have tested proximal-layer corrections[12] to the SST for polymer brushes against SCFT predictions. These corrections alone resolve, at least qualitatively, a severe discrepancy between the self-consistent fields, $w(z)$, predicted by SST and SCFT. They also account for a nonzero slope in the individual polymer profiles at the substrate as predicted by SCFT. When combined with end-segment-entropy corrections,[8] the agreement with SCFT becomes impressive, particularly in regards to $w(z)$ but also in regards to the stretching energy of the individual chains, $f_{0,e}(z_0)$.

In the case of the two opposing brushes examined here, there still remains a sizable discrepancy between SST and SCFT regarding the degree to which the segment profiles of the two brushes interpenetrate.[8] This will of course require another correction that accounts for fluctuations about the classical trajectories. Once this is taken care of, it would be useful to extend these studies to other systems involving, for example, curved substrates, added solvents, homopolymers, etc. Experience has shown that detailed investigations of this nature have a habit of turning up valuable insights into polymeric behavior.

ACKNOWLEDGMENTS

We are grateful to Sasha Semenov for discussions regarding some of the unpublished details of Ref. 12. This work was supported by the EPSRC (GR/M61160).

[1] S. T. Milner, Science **251**, 905 (1991).
[2] M. Doi and S. F. Edwards, *The Theory of Polymer Dynamics* (Clarendon, Oxford, 1986).
[3] S. F. Edwards, Proc. Phys. Soc. London **85**, 613 (1965).
[4] M. W. Matsen and J. M. Gardiner, J. Chem. Phys. **115**, 2794 (2001).
[5] P. G. Ferreira, A. Ajdari, and L. Leibler, Macromolecules **31**, 3994 (1998).
[6] A. N. Semenov, Sov. Phys. JETP **61**, 733 (1985).
[7] S. T. Milner, T. A. Witten, and M. E. Cates, Macromolecules **21**, 2610 (1988).
[8] M. W. Matsen, J. Chem. Phys. **117**, 2351 (2002).
[9] M. W. Matsen and F. S. Bates, Macromolecules **28**, 8884 (1995).
[10] S. T. Milner, J. Chem. Soc., Faraday Trans. **86**, 1349 (1990).
[11] J. L. Goveas, S. T. Milner, and W. B. Russel, Macromolecules **30**, 5541 (1997).
[12] A. E. Likhtman and A. N. Semenov, Europhys. Lett. **51**, 307 (2000).